UDK 620.3:669.75:669.6:66.017
Original scientific article/Izvirni znanstveni članek

ISSN 1580-2949
MTAEC9, 55(5)667(2021)

PREPARATION OF ATO NANOPOWDERS WITH Co-PRECIPITATION AND THEIR LASER-REFLECTION PROPERTIES

PRIPRAVA NANODELCEV KOSITER-ANTIMONOVEGA OKSIDA S KOPRECIPITACIJO IN NJIHOVE LASERSKE ODBOJNE LASTNOSTI

Jing Zhang*

Wuxi Vocational Institute of Arts & Technology, Yixing 214209, China

Prejem rokopisa – received: 2020-07-12; sprejem za objavo – accepted for publication: 2021-07-01

doi:10.17222/mit.2020.228

Antimony tin oxide (ATO) nanoparticles were prepared using co-precipitation with tin chloride and antimony chloride as the main raw materials. X-ray diffraction (XRD), field-emission scanning electron microscopy (FESEM) and ultraviolet-visible spectrophotometry were used to characterize the crystal structure, morphology and laser reflectivity. The effects of the pH value, co-precipitation reaction temperature, calcination temperature and calcination time on the laser reflectivity of ATO nanoparticles were studied. The results show that, compared with the undoped SnO_2 powder, the reflectivity of a Sb-doped ATO powder at a laser wavelength of 1.06 μm is significantly reduced, and with an increase in the Sb doping, the reflectivity of the ATO powder at 1.06 μm first decreases and then increases. When the Sb/Sn molar ratio is 2/10, the reflectivity decreases to the lowest point, which is caused by the high concentration of Sb^{5+}. ATO powders (Sb/Sn = 2/10) prepared at a titration-end-point pH of 2, co-precipitation temperature of 70 °C, calcination temperature of 800 °C and calcination time of 6 h have the lowest laser reflectivity at the laser wavelength of 1.06 μm, which is less than 0.02 %.

Keywords: antimony tin oxide, laser reflectivity, preparation technology

V članku so predstavljeni kositer-antimonov oksidni (ATO) nanodelci prahu s postopkom koprecipitacije (slov. izločanja) z uporabo izhodnih surovin kositrovega in antimonovega klorida. Iz nastalih nanodelcev je bila, s pomočjo rentgenske difrakcije (XRD), vrstične elektronske mikroskopije na emisijo polja (FE/SEM) in spektrometra na vidno in ultravijolično svetlobo, določena kristalna struktura, morfologija in odbojnost prahu za lasersko svetlobo. Obravnavan je tudi vpliv kislosti raztopine (pH), temperatura koprecipitacijske reakcije in temperatura ter čas kalcinacije na reflektivnost ATO nano-delcev. Rezultati raziskave so pokazali, da imajo delci dopirani z antimonom (Sb), v primerjavi s čistim SnO_2 prahom, bistveno manjšo reflektivnost laserske svetlobe z valovno dolžino 1,06 μm in da z naraščajočo vsebnostjo Sb odbojnost ATO prahu najprej pada in nato zopet narašča. Pri molarnem razmerju Sb/Sn je 2/10 je odbojnost padla na najnižjo vrednost zaradi velike koncentracije Sb^{5+} ionov. ATO prahovi (Sb/Sn = 2/10), izdelani na koncu titracije pri pH = 2, temperaturi koprecipitacije 70 °C, temperaturi kalcinacije 800 °C in času kalcinacije 6 ur, imajo najmanjšo (0,02 %) odbojnost laserske svetlobe z valovno dolžino 1,06 μm.

Ključne besede: kositer-antimonov oksid, tehnologija izdelave, odbojnost laserske svetlobe

1 INTRODUCTION

At present, the laser stealth is mainly aimed at 1.06 μm and 10.6 μm laser wavelengths. Laser stealth is achieved by reducing the reflectivity at these two laser wavelengths.[1] The level of science and technology determines the development of a war situation and military strength of a country; thus, the influence of advanced weapons on future wars is more and more important. With the application of advanced detection equipment operating in various wavebands, individual stealth materials cannot meet the stealth needs of modern war, so the stealth material is developing towards a multi-spectrum stealth material that can be compatible with multi-band electromagnetic wave stealth, such as meter wave, centimeter wave, millimeter wave, infrared, laser and so on. Near-the-plasma oscillation frequency, an absorption peak induced by an incident photon and plasma resonance appears because of the special optical properties of semiconductor materials.[2] When the wavelength of the incident light is lower than the plasma wavelength of a semiconductor, the incident light can propagate in the medium. Therefore, by doping, the carrier concentration can be controlled to change the plasma wavelength of the doped semiconductor compound so that it can produce strong absorption near the wavelength of 1.06 μm. At the same time, the infrared radiation range of a doped semiconductor compound can be separated from the infrared atmospheric window with a doping modification so that the infrared and laser compound stealth abilities are compatible. Therefore, a doped semiconductor compound can be used as one of the functional materials for laser stealth.[3,4] Antimony tin oxide (ATO) is a common doped semiconductor material. It exhibits strong absorption of the 1.06 um laser, so it has low reflectivity at the 1.06 um laser wavelength. It is a laser-stealth material

*Corresponding author's e-mail:
zhangjing_20062007@126.com (Jing Zhang)

with good development prospects. Nano-ATO also has many excellent properties, such as high transparent conductivity, excellent optical properties and good weather resistance.[5,6] Thus, it can be widely used for the preparation of electrode materials, transparent heat-insulation materials, infrared-absorption materials and so on.[7,8]

However, there are few related studies and reports on ATO as a laser-stealth material.[9,10] N. Haddad and other authors[11] prepared ATO using a facile sol-gel method; their results suggested that the as-prepared ATO nanoparticles were a good quality material for thin-film solar-cell applications. Abhijit A.Yadav[12] prepared transparent conducting antimony-doped SnO_2 thin films with chemical spray pyrolysis; the results showed that the average optical transmittance of the films decreased from 89 % to 73 % within the visible range of 350–850 nm with an increase in the film thickness. The preparation methods for nanopowders are various.[13,14] Among them, co-precipitation is a better method for preparing ATO nanopowders because of its simple operation, easy control of the process flow and homogeneous preparation of nanopowders.[15] In this paper, ATO powders were prepared with the co-precipitation method. The plasma frequency, visible-light and near-infrared transmittance as well as infrared reflectivity of the ATO powders are all related to the main phase, doped phase and preparation process of the doped semiconductor. Through research, analysis and selection, the best values of the carrier concentration, conductivity and dielectric constant can be obtained.

2 EXPERIMENTAL PART

2.1 Preparation of the ATO powder with co-precipitation

The main raw materials of this experiment were tin tetrachloride, antimony trichloride, ammonia water and concentrated hydrochloric acid. Tin tetrachloride and antimony trichloride were weighed proportionally and placed in a beaker. A certain amount of a 1:1 hydrochloric acid solution was added to the beaker. The solution was fully stirred and dissolved to form a transparent solution. Ammonia water was added to the transparent solution drop by drop as the precipitant. The pH value was adjusted by controlling the amount of ammonia droplets to produce a co-precipitation reaction. The co-precipitation reactants were aged for a period of time, washed with deionized water and ethanol for several times, and then dried in an oven at 80 °C. The dried ATO precursor was ground and calcined in a resistance furnace to obtain ATO powder.

2.2 Analysis and characterization

The phase composition of the sample powder was analyzed with an ARL X'TRA X-ray diffractometer from the American Thermo Electric Company. The test conditions were as follows: a Cu-K_α ray and a 2θ angle scanning range of 10–70°. The phase composition, crystal structure, cell parameters and grain size of the ATO powder were analyzed with the MDI Jade 5.0 software. The morphology of the samples was analyzed with a LEO-1530VP field-emission scanning electron microscope (FESEM) from LEOL Company, Japan. The reflectance spectra of the samples in the wavelength range of 900–1800 nm were measured with a UV-3101PC ultraviolet, near-infrared spectrophotometer made by Shimadzu Company, Japan, and the reflectivity of the samples at the 1.06 μm laser wavelength was recorded.

3 RESULTS AND DISCUSSION

3.1 The pH value

In the co-precipitation liquid system, the pH value of the solution is one of the main influencing factors. In order to complete the co-precipitation reaction and if the precipitation particles generated are not too small to be filtered, the pH value of the titration end-point solution should be adjusted in a range of 2–6. Under the same co-precipitation temperature, a Sb/Sn molar ratio of 2/10, calcination temperature of 600 °C and calcination time of 2 h, the pH value of the titration end-point solution was set to 2, 4 and 6. The ATO powders prepared were tested with XRD and the results are shown in **Figure 1**. **Figure 1** shows that with a decrease in the pH value, the intensity of a diffraction peak increases and the diffraction peak sharpens. When the pH value decreases from 6 to 2, the crystallization degree of an ATO powder increases gradually.

The laser reflectivity of the ATO powders prepared at different pH values was measured and analyzed with the ultraviolet-visible-infrared spectrophotometer. The reflectance map is shown in **Figure 2**. **Figure 2** shows that the ATO powders prepared at different pH values have very low reflectivity in the near-infrared band of

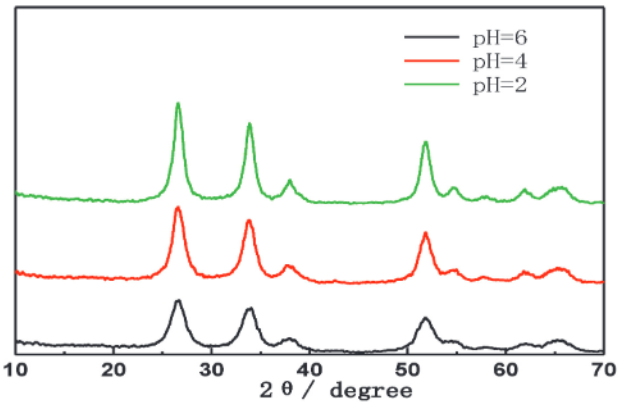

Figure 1: XRD patterns of ATO powders obtained with different pH values. Preparation conditions: Sb/Sn molar ratio of 2/10, reaction temp. = normal temp., calcination temperature of 600 °C, calcination time of 2 h

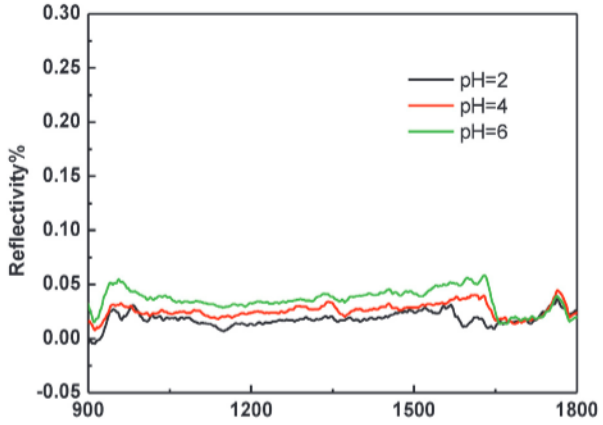

Figure 2: Reflectivity curves of ATO powders obtained with different pH values

900–1800 nm (covering the 1.06 μm laser wavelength), which indicates that the ATO powders exhibit strong absorption at the 1.06 μm laser wavelength. With the decrease in the pH value, the reflectivity of the ATO powder decreases further. When the pH value is 2, the reflectivity of the ATO powder at the 1.06 μm laser wavelength reaches the lowest value of about 0.03 %. This might be due to a uniform distribution of precipitation and doping, an increase in the grain size of the ATO powders and a better crystallinity at a low pH value. However, when the pH value is high, the precipitation reaction is too fast and the doping distribution is not uniform, which reduces the carrier transition probability of the donor level; therefore, the carrier absorption performance in the near-infrared region is weakened, and the reflectance at the 1.06 μm laser wavelength is increased.

3.2 Co-precipitation reaction temperatures

The co-precipitation temperature will affect the rate of precipitation reaction and the heat treatment temperature, which will affect the performance of ATO powder. The laser reflectivity of ATO powders prepared at different co-precipitation temperatures of 30 °C, 50 °C and 70 °C was measured and analyzed by ultraviolet-visible-infrared spectrophotometer. The reflectivity map is shown in **Figure 3**. As can be seen from **Figure 3**, the reflectivity of ATO powder at the 1.06 μm laser wavelength decreases with the increase of co-precipitation temperature. The laser reflectivity of ATO powder prepared for the co-precipitation temperature of 70 °C is the lowest, which is about 0.03 %. It may be due to the improvement of crystallinity of ATO powder with the increase of co-precipitation temperature and grain size.

3.3 Calcination temperatures

The precursor powder ATO was calcined at (300; 400; 500; 600; 700 and 800) °C. **Figure 4** shows the reflectance spectra of the ATO powders prepared with a spectrophotometer at the calcination temperatures of (300; 400; 500; 600; 700 and 800) °C. The reflectivity of the ATO powders at the 1.06 μm laser wavelength is about 0.06 % when calcined at 300 °C. With the increase in the calcination temperature, the reflectivity decreases gradually. The reflectivity of the ATO powders prepared with calcination at 800 °C decreases to about 0.03 %. This is due to the increase in the number of Sb^{3+} converted to Sb^{5+} after the calcination-temperature increase, leading to an increase in the carrier concentration in ATO and an easier electronic transition of the donor level. Therefore, the absorption at the 1.06 μm laser wavelength is enhanced and the reflectivity is reduced.

3.4 Calcination time

The ATO precursors were calcined at 800 °C for (2; 4; 6) h. The effect of the calcination time on the laser-stealth performance of an ATO powder was discussed. **Figure 5** shows the XRD spectra of the ATO powders calcined at different times. It can be seen from **Figure 5** that with the increase in the calcination time,

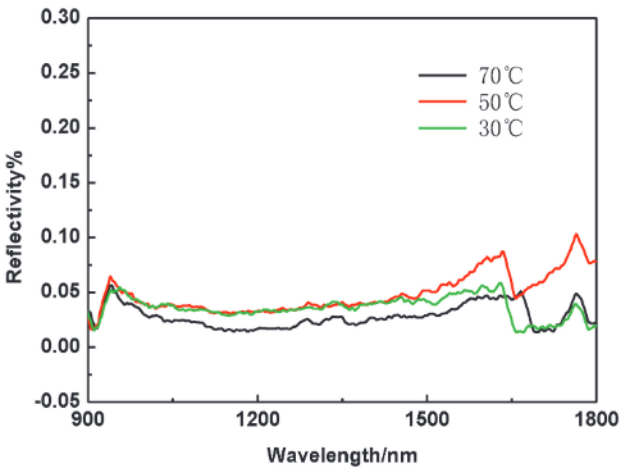

Figure 3: Reflectivity curves of ATO powders obtained with different reaction temperatures

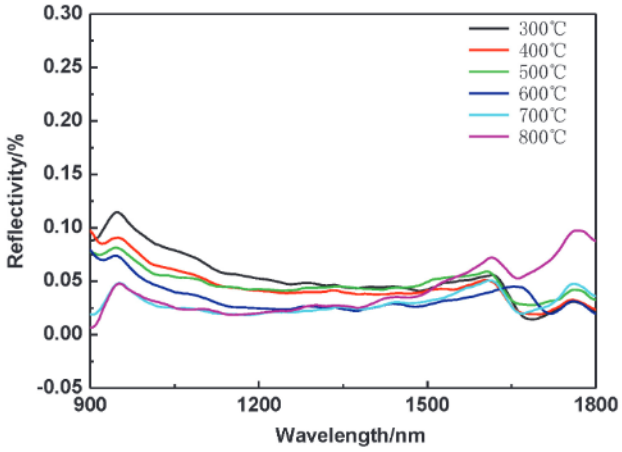

Figure 4: Reflectivity curves of ATO powders obtained at different calcination temperatures. Preparation conditions: Sb/Sn molar ratio of 2/10, pH = 2, reaction temp. = normal temp., calcination time of 2 h

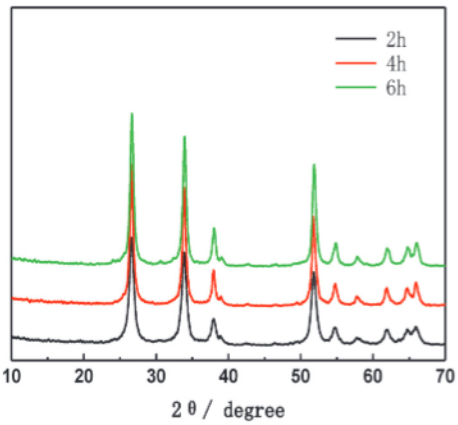

Figure 5: XRD patterns of ATO powders obtained at different calcination times. Preparation conditions: Sb/Sn molar ratio of 2/10, pH = 2, reaction temperature of 70 °C, calcination temperature of 800 °C

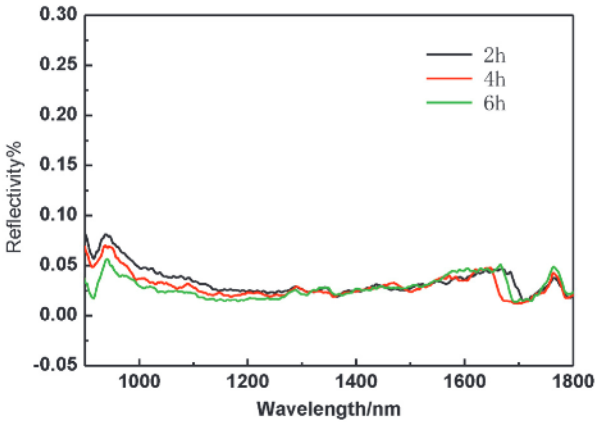

Figure 7: Reflectivity curves of ATO powders obtained at different calcination times

the intensity of diffraction peaks increases and the shape of the peaks becomes sharper.

The FE-SEM photographs of the ATO powders calcined at different times are shown in **Figure 6**. It can be seen that the ATO powders prepared at different calcination times exhibit a certain agglomeration phenomenon, showing irregular spherical shapes. With the extension of the calcination time, the primary-particle size gradually grows up. When calcined for 2 h, the primary-particle size is about 60 nm; and when calcined for 4 h, the primary-particle size is about 80 nm. When the calcination time is extended to 6 h, the primary-particle size is about 100 nm.

The laser reflection of the ATO powders prepared with calcination at different times was tested and analyzed with an ultraviolet-visible-infrared spectrophotometer. The reflection spectra are shown in **Figure 7**. It can be seen from **Figure 7** that a proper prolongation of the calcination time is beneficial for further reduction of reflectivity. After the calcination for 6 h, the reflectivity decreases to about 0.02 %. The scattering extinction effect of the ATO powders at the 1.06 μm laser wavelength is enhanced and the reflectivity is reduced due to the increase in the particle size caused by the prolongation of the calcination time. However, the low reflectivity of the ATO powders at the 1.06 μm laser wavelength is mainly due to the fact that ATO is a material with a strong absorption of the 1.06 μm laser light, so the effect of the particle-size change on the reflectivity is not very big.

3.5 Influence of the Sb content

The effect of the Sb doping on the structure of an ATO powder was investigated when the Sb/Sn molar ratio was set to 0/10, 1/10, 2/10 and 3/10. The XRD test results are shown in **Figure 8**. After the calcination at 800 °C, all the ATO powders with different Sb/Sn molar ratios show the characteristic diffraction peaks of SnO_2, and there are no other characteristic diffraction peaks of a crystalline phase, indicating that the ATO-powder structure is still a rutile structure of tetragonal SnO_2, but the diffraction-peak intensity of the SnO_2 doped with Sb is lower than that of undoped SnO_2, and the diffraction peaks of the (112) and (301) crystal planes have not yet appeared. At the same time, with an increase in the Sb doping amount to 2/10, the intensity of diffraction peaks is further reduced, and the diffraction peaks are widened in varying degrees. This is because after Sb partially replaces Sn, lattice defects are caused, hindering the growth rate of ATO grains, leading to a decrease in the grains and the broadening of diffraction peaks.

The laser reflection of the ATO powders with different Sb contents was tested and analyzed with a ultraviolet-visible-infrared spectrophotometer. **Figure 9** shows the reflectivity of the ATO powders with different Ab-doping amounts. Compared with the undoped SnO_2

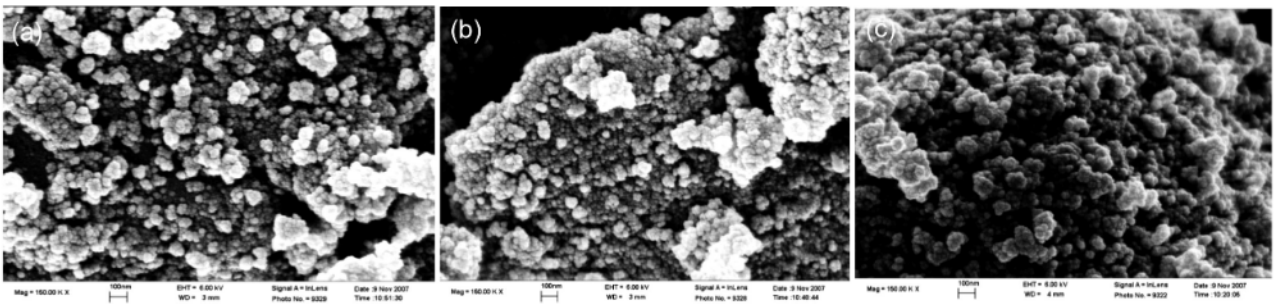

Figure 6: FE-SEM images of ATO powders obtained at different calcination times

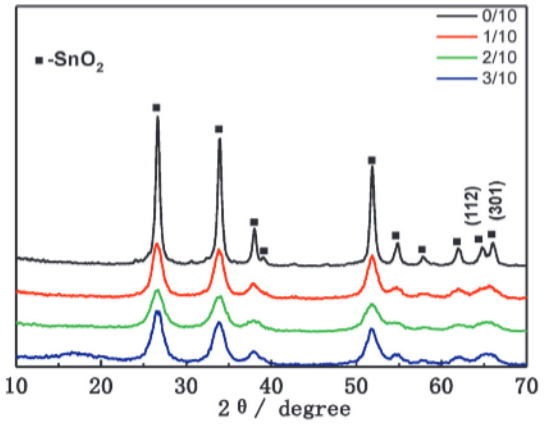

Figure 8: XRD patterns of ATO powders obtained at various Sb/Sn molar ratios. Preparation conditions: calcination temperature of 800 °C, pH = 2, reaction temp. = normal temp.

powder, the reflectivity of the Ab-doped ATO powder at the 1.06 μm laser wavelength is significantly lower. After the Sb doping, Sb^{5+} enters SnO_2 instead of Sn^{4+}, producing a positive charge center. The excess electrons form the donor impurity energy level near the bottom of the conduction band. The number of carriers increases greatly, resulting in the plasma exciton effect, and the near-infrared band (covering 1.06 μm) absorption increases greatly. With the increase in the Sb/Sn molar ratio, the reflectivity first decreases and then increases. When the Sb/Sn molar ratio is 2/10, the reflectivity of the ATO powder at the laser wavelength of 1.06 μm decreases to the lowest point. However, when Sb doping continues to increase, the ratio of Sb^{5+}/Sb^{3+} decreases, Sb^{3+} takes the place of Sn^{4+}, and Sb^{3+} forms the acceptor energy level, which compensates for part of the electrons generated by Sb^{5+}, reducing the effective carrier concentration so that the reflectivity of the ATO powder at the laser wavelength of 1.06 μm is relatively high.

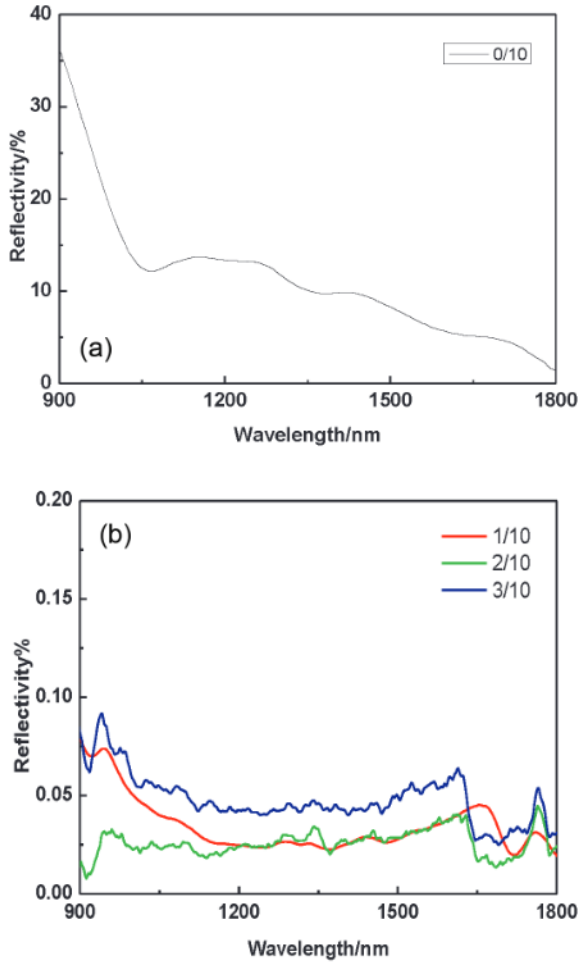

Figure 9: Reflectivity curves of ATO powders obtained at various Sb/Sn molar ratios

4 CONCLUSIONS

The crystal structure, particle size and laser reflectivity of the ATO powders prepared with the co-precipitation method are affected by the preparation conditions (co-precipitation reaction temperature, calcination temperature/time and titration-end-point pH). The reflectivity of the Sb-doped ATO powder at the laser wavelength of 1.06 μm is significantly lower than that of undoped SnO_2 powder, and with an increase in the Sb doping, the reflectivity of the ATO powders at 1.06 μm first decreases and then increases. When the Sb/Sn molar ratio is 2/10, the reflectivity decreases to the lowest point, which is due to a high concentration of Sb^{5+}. From the point of view of the preparation technology, the 1.06 μm laser reflectivity of the ATO powders (Sb/Sn = 2:10), prepared under conditions of a titration-end-point pH of 2, co-precipitation temperature of 70 °C, calcination temperature of 800 °C and calcination time 6 h, is less than 0.02 %.

Acknowledgements

This work was financially supported by the General Projects of Natural Science Research in Jiangsu Universities in 2020 (20KJB430028) and the "Blue Project" of Jiangsu Universities.

5 REFERENCES

[1] X. L. Chen, C. H. Tian, T. P. Chen, Composite grating structure for laser and infrared compatible stealth with high visible transmittance, Optik, 183 (**2019**), 863–868, doi:10.1016/j.ijleo.2019.03.007

[2] V. A. Saveleva, L. Wang, O. Kasian, M. Batuk, J. Hadermann, J.-J. Gallet, F. Bournel, N. Alonso-Vante, G. Ozouf, C. Beauger, K. J. J. Mayrhofer, S. Cherevko, A. S. Gago, K. A. Friedrich, S. Zafeiratos, E. R. Savinova, Insight into the Mechanisms of High Activity and Stability of Iridium Supported on Antimony-Doped Tin Oxide Aerogel for Anodes of Proton Exchange Membrane Water Electrolyzers, ACS Catalysis, 10 (**2020**) 4, 2508–2516, doi:10.1021/acscatal.9b04449

[3] Y. S. Qin, M. J. Zhang, Y. Guan, X. G. Huang, Laser absorption and infrared stealth properties of Al/ATO composites, Ceramics International, 45 (**2019**) 11, 14312–14315, doi:10.1016/j.ceramint.2019.04.144

[4] Z. Qiu, Z. F. Xiao, L. K. Gao, J. Li, H. G. Wang, Y. G. Wang, Y. J. Xie, Transparent wood bearing a shielding effect to infrared heat and ultraviolet via incorporation of modified antimony-doped tin oxide nanoparticles, Composites Science Technology, 172 (**2019**), 43–48, doi:10.1016/j.compscitech.2019.01.005

[5] S. Sreekumar, A. Joseph, C. S. Sujith Kumar, S. Thomas, Investigation on influence of antimony tin oxide/silver nanofluid on direct absorption parabolic solar collector, Journal of Cleaner Production, 249 (**2020**), 119378, doi:10.1016/j.jclepro.2019.119378

[6] G. H. Fan, Z. Y. Wang, K. Sun, Y. Liu, R. H. Fan, Doping-dependent negative dielectric permittivity realized in mono-phase antimony tin oxide ceramics, Journal of Materials Chemistry C, 8 (**2020**), 11610–11617, doi:10.1039/D0TC02266G

[7] B. Khorshidi, S. A. Hosseini, G. Ma, M. McGregor, M. Sadrzadeh, Novel nanocomposite polyethersulfone-antimony tin oxide membrane with enhanced thermal, electrical and antifouling properties, Polymer, 163 (**2019**), 48–56, doi:10.1016/j.polymer.2018.12.058

[8] J. Zhang, Y. D. Sun, J. S. Xu, Fabrication of antimony doped tin oxide nanopowders as an advanced electrode material for supercapacitors, Micro & Nano Letters, 14 (**2019**) 3, 254–258, doi:10.1049/mnl.2018.5212

[9] J. Zhang, L. X. Wang, Q. T. Zhang, Influence of Sb content on electromagnetic properties of ATO/ferrite composites synthesized by co-precipitation method, Journal of Magnetism and Magnetic Materials, 390 (**2015**), 107–113, doi:10.1016/j.jmmm.2015.04.079

[10] J. Zhang, L. X. Wang, M. P. Liang, Q. T. Zhang, Effects of Sb content on structure and laser reflection performance of ATO nanomaterials, Transactions of Nonferrous Metals Society of China, 24 (**2014**) 1, 131–135, doi:10.1016/S1003-6326(14)63038-7

[11] N. Haddad, Z. Ben Ayadi, K. Djessas, Synthesis and characterization of antimony doped tin oxide aerogel nanoparticles using a facile sol–gel method, Journal of Materials Science: Materials in Electronics, 29 (**2018**) 1, 721–729, doi:10.1007/s10854-017-7965-4

[12] A. A. Yadav, Influence of film thickness on structural, optical, and electrical properties of spray deposited antimony doped SnO_2 thin films, Thin Solid Films, 591 (**2015**), 18–24, doi:10.1016/j.tsf.2015.08.013

[13] C. L. Wang, D. Wang, R. Q. Yang, H. F. Wang, Preparation and electrical properties of wollastonite coated with antimony-doped tin oxide nanoparticles, Powder Technology, 342 (**2019**), 397–403, doi:10.1016/j.powtec.2018.09.092

[14] S. D. Ponja, B. A. D. Williamson, S. Sathasivam, D. O. Scanlon, I. P. Parkin, C. J. Carmalt, Enhanced electrical properties of antimony doped tin oxide thin films deposited via aerosol assisted chemical vapour deposition, Journal of Materials Chemistry C, 6 (**2018**), 7257–7266, doi:10.1039/C8TC01929K

[15] T. Krishnakumar, R. Jayaprakash, N. Pinna, A. R. Phani, M. Passacantando, S. Santucci, Structural, optical and electrical characterization of antimony-substituted tin oxide nanoparticles, Journal of Physics and Chemistry of Solids, 70 (**2019**) 6, 993–999, doi:10.1016/j.jpcs.2009.05.013